View metadata, citation and similar papers at core.ac.uk

brought to you by CORE

provided by Missouri University of Science and Technology (Missouri S&T): Scholars' Mine

Missouri University of Science and Technology

Scholars' Mine

International Conference on Case Histories in Geotechnical Engineering

(1984) - First International Conference on Case Histories in Geotechnical Engineering

11 May 1984, 8:00 am - 10:30 am

# Settlements Induced by Soft Ground Tunneling

Miguel P. Romo

*Universidad Nacional de México, México*

Follow this and additional works at: https://scholarsmine.mst.edu/icchge

 Part of the Geotechnical Engineering Commons

## Recommended Citation

Romo, Miguel P., "Settlements Induced by Soft Ground Tunneling" (1984). *International Conference on Case Histories in Geotechnical Engineering*. 39.
https://scholarsmine.mst.edu/icchge/1icchge/1icchge-theme9/39

This Article - Conference proceedings is brought to you for free and open access by Scholars' Mine. It has been accepted for inclusion in International Conference on Case Histories in Geotechnical Engineering by an authorized administrator of Scholars' Mine. This work is protected by U. S. Copyright Law. Unauthorized use including reproduction for redistribution requires the permission of the copyright holder. For more information, please contact scholarsmine@mst.edu.

# Settlements Induced by Soft Ground Tunneling

**Miguel P. Romo**

**Research Professor, Instituto de Ingeniería, Universidad Nacional de México, México, D.F.**

SYNOPSIS Ground settlements induced by air-pressure shield tunneling throughout the soft clays of Mexico City have been monitored in five test sections by means of settlement points installed at various depths and distances from the tunnel axis. Subsoil conditions and soil characteristics at each site were thoroughly studied in the field and in the laboratory. Measured settlement profiles have been compared to those computed by a simplified analytical procedure showing very good agreement.

## INTRODUCTION

Recent investigations by Romo et al. (1979), Reséndiz and Romo (1981), and Romo (1983), have led to the development of a simplified procedure to predict settlements caused by pressurized shield tunneling operations. This method includes the stress-strain-strength characteristics of the subsoil, air pressure, free field conditions, and the geometry of the tunnel-soil system. Furthermore, computation of settlements due to different stages during construction can be achieved directly and, hence, practical recommendations to decrease soil movements may result from the application of the method.

With the aim of gaining experience and confidence in the method, a number of test sites have been set up along the path of deep sewer tunnels running through soft clay. Five of these test sites are reported in this paper. Field measurements were carried out by means of accurate surveyings run as often as twice a day (when tunneling was going on nearby testing sites), with the purpose of beeing able to discern the effect of the various construction stages such as front excavation, shield shoving, and primary lining set up.

In this paper, the simplified method modified by Romo (1983) is used to compute settlement profiles at five instrumented sections and compared to the corresponding measured vertical soil movements. On the basis of these results, conclusions regarding the suitability of the method and its potential use as a tool to helping design soft ground tunnels are reached.

## NEED FOR PREDICTING SETTLEMENT PROFILES

Construction of tunnels in soft ground necessarily cause ground movements and, consequently, soil strains which in turn can damage neighboring buildings and line services.

The design engineer of tunnels in urban areas should be able to predict the consequences of the excavation with regard to construction method, ease of work at tunnel face and potential damage at ground level. Having a reliable prediction of the spatial distribution of settlements (and strains) along the tunnel path, the engineer would be in an advantageous position to modify construction procedures in such a way that settlements be reduced to tolerable levels.

There are situations where construction procedure changes or modifications to tunnel alignment are not feasible. In these cases, knowing the potential settlement profiles the behavior of neighboring structures and line services can be assessed and pertinent precautions taken.

As noted by Attewell (1981), another reason for wanting to know the distribution and magnitude of settlements is of contractual type.

## TUNNEL CHARACTERISTICS

The tunnel, Fig. 1, extends 1888 m in the zone of the lake, as defined by Marsal and Mazari (1959), at an average depth of its axis of 23 m. The tunnel was advanced from shaft number 6 to shaft 7 (see Fig. 1), and was excavated by full-face hand mining under compressed air through basically soft clay, as shown in Fig. 2.

The construction procedure included a 6.24 m diameter shield and a compressed air system capable of reaching pressures up to 1.5 kg/cm$^2$, according to Schmitter et al. (1981). The primary lining consisted of precast segments 75 cm long and 25 cm thick. Each ring of precast segmented lining consisted of four segments which were assembled in the shield behind the mole. Every ring is pushed out of the shield when this has advanced beyond that ring and the void left between ring and excavated soil is grouted with pea gravel.

The main stages involved in the construction pro-

cedure adopted along the tunnel where the test sections were set up were: a) tunnel stabilization with an open face shield and compressed air, b) advancement of the shield with jacks reacting against the primary lining already installed, c) installation of an additional ring of precast segmented lining (primary or temporary) behind the shield tail, and d) injection of pea gravel and grouting to fill up the gap left between lining and tunnel wall. The air pressure was kept constant within the pressurized chamber until works to build up the secondary (or permanent) lining were initiated.

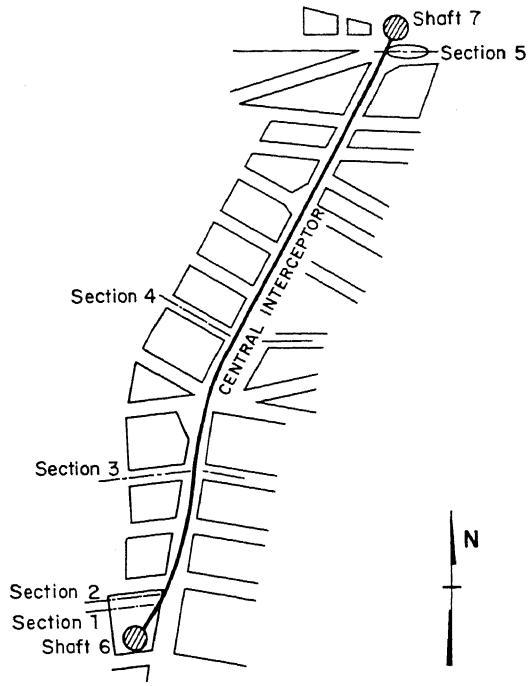


Fig. 1. Central Interceptor Tunnel

TEST SECTIONS

The general lay out of the five instrumented sections is shown in Fig. 1. The first two were set up in a park, the third and fourth at insersections with wide streets, and the fifth on a traffic circle.

The instrumentation consisted of settlement points buried at different depths. The subsoil investigations included cone penetration tests and laboratory testing of undisturbed samples. The ground water surface was found about 3 m deep in all sites.

Sections 1 and 2

These two sections are some 20 m apart from each other and are located in a park. The subsoil conditions representative of the site are shown in Fig. 3. From 0 to 5 m (not shown in Fig. 3) artificial fill and dissicated sandy clay materials were found; then comes a layer 3 m thick of overconsolidated clay followed by two sand layers sandwiching a normally consolidated clay layer. Underlying these layers, there is a 20 m-thick stratum of normally consolidated clay with intercalated seams of silty clay, fosils, fly ashes, and hardened clay (probably by dissication). Natural water contents with depth are also included in Fig. 3.

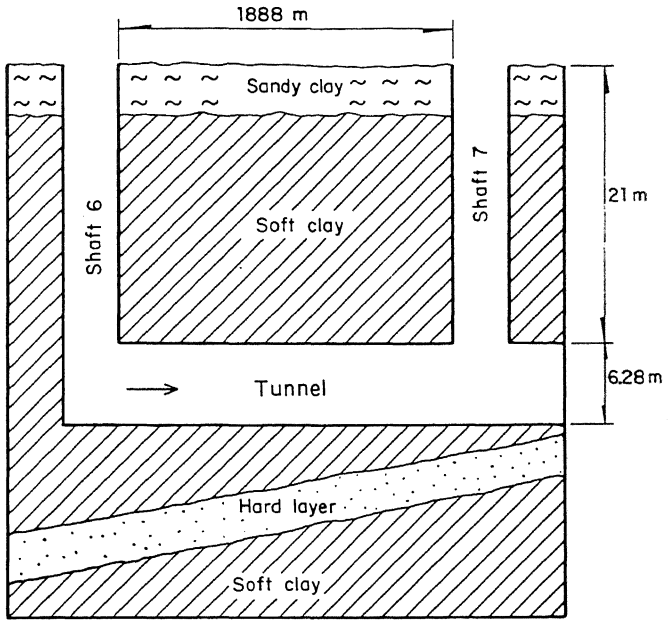


Fig. 2. Longitudinal Section of Central Interceptor Tunnel

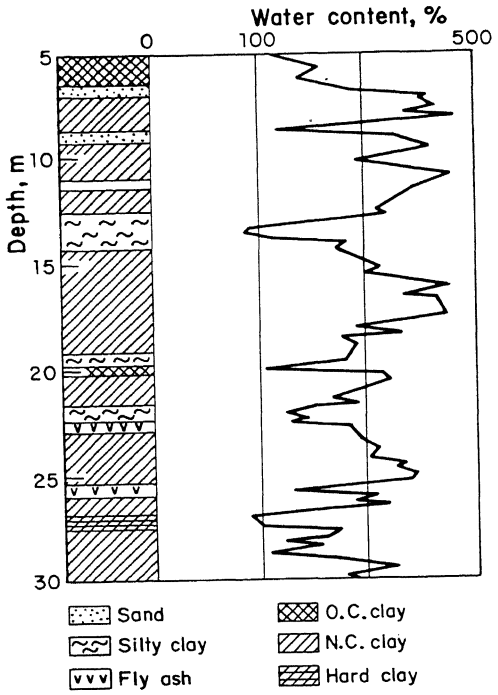


Fig. 3. Soil Profile at Sections 1 and 2

The cone and sampling borings were made somewhere at mid distance between the two instrumented sections and some 2 m apart from each other. Cone point resistance was measured at a driving rate of 2 cm/sec. The corresponding undrained strength versus depth is shown in Fig. 4. Alternatively, undrained triaxial tests (UU) were carried out on the undisturbed samples. The laboratory undrained strengths were correlated with those obtained by means of the cone. The resulting parameter N was 13 for soft layers (i.e., cone point resistance less than about 10) and 24 for hard layers (i.e., cone point resistance greater than about 15). The resulting correlation between cone resistance for these values of N is shown in Fig. 4.

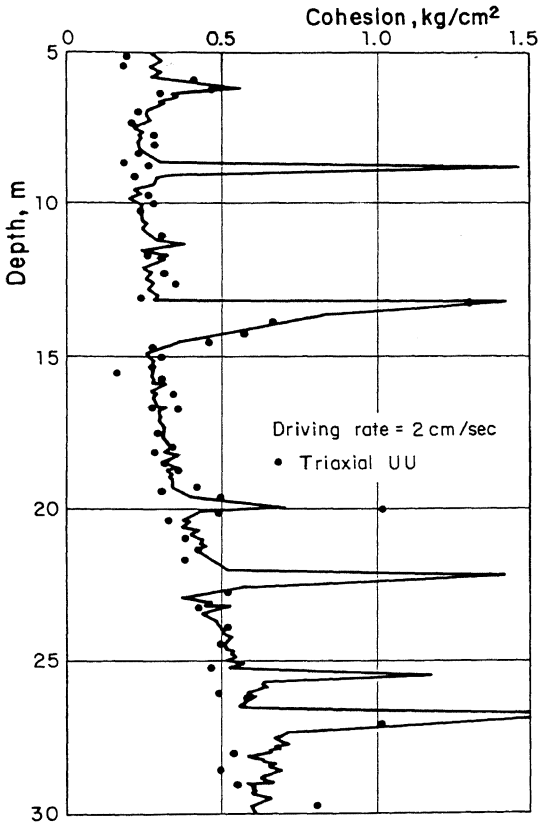


Fig. 4. Cone and Laboratory Undrained Resistances. Sections 1 and 2

Correlations of the type shown in Fig. 4 are very useful when it comes to predict tunneling-induced settlements as will be shown later.

Stress-strain curves obtained from the triaxial testing program, allowed computation of average values of the initial tangent modulus, $E_i$, and of the shear strength ratio, $R_f$. These values along with average values of shear strength, $\sigma_f$, and unit weight, $\gamma$, are presented in Table I.

TABLE I. Average Soil Characteristics. Sections 1 and 2

| Layer | $E_i$ (t/m²) | $R_f$ | $\sigma_f$ (t/m²) | $\gamma$ (t/m³) |
|---|---|---|---|---|
| from 6.5 m to 12.5 m | 630 | 0.88 | 6.0 | 1.2 |
| from 12.5 m to 20.5 m | 600 | 0.90 | 6.5 | 1.2 |

In addition to stress-strain-strength characteristics, the method of analisis used in this paper requires the knowledge of the soil compressibility in its undisturbed and remolded states. To this end, oedometer tests were carried out on samples obtained from the clay layer above the tunnel crown. Compressibility curves (shown in Fig. 5) were determined for both conditions of two contiguous samples having equal water content. Determinations of water content before and after remolding showed no appreciable water loss. Accordingly, disturbed and undisturbed samples were equivalent and the differences in their compressibility curves may be thought to be caused by sample remolding solely.

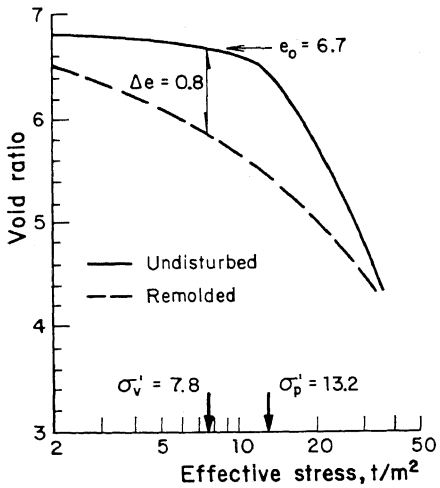


Fig. 5. Representative Compressibilities of Sections 1 and 2

Instrumentation at these two sections consisted of 16 settlement points distributed in space as shown in Fig. 6. Eight of the settlement points were installed at a depth of 6.5 m, and the remaining eight at 12.5 m. Two of the measuring points were located above tunnel axis and the remaining at varying horizontal distances to define better the settlement profiles.

Section 3

This field station was located at the intersection of two wide avenues. The subsoil characteristics of the site are shown in Fig. 7. The stratigraphy is similar to that of sections 1 and 2: from 0 to 5 m (not shown in Fig. 7) artificial fill and dissicated sandy clay materials were found; then comes a layer about 2 m thick of over consolidated clay followed by a thin layer of sand. Underlying these layers, there is a 23 m-thick stratum of normally consolidated clay with intercalated seams of silty clay fosils, fly ashes, and hardened clay (possibly by dissication). Natural water content ranged between 20% to more than 500%; the profile of water content is shown in Fig. 7.

The cone and sampling borings were carried out some twelve meters from tunnel axis and one meter a way from the line of settlement points. Cone point resistance was measured at a driving rate of 2 cm/sec. The resulting undrained strength versus depth is included in Fig. 8. Alternatively, undrained triaxial tests (UU) were performed on undisturbed samples. The resulting undrained strengths were correlated with the corresponding strengths obtained by means of the cone penetration test. The correlation parameter N was 15 for soft layers (i.e., cone point resistance less than about 10) and 21 for harder layers (i.e., cone point resistance greater than about 15). Such correlation between cone resistance and UU resistance is shown in Fig. 8.

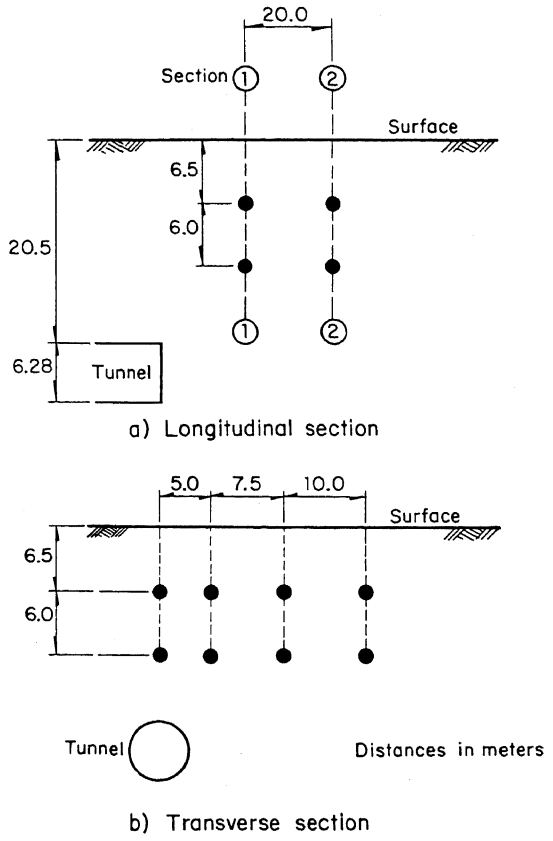


Fig. 6. Spatial Distribution of Settlement Points. Sections 1 and 2

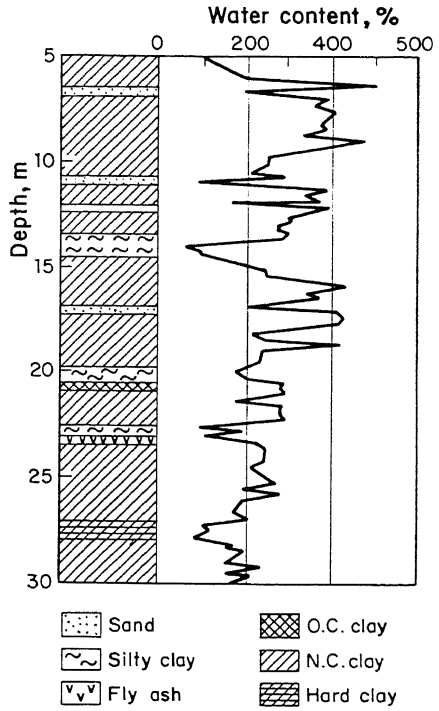


Fig. 7. Soil Profile at Section 3

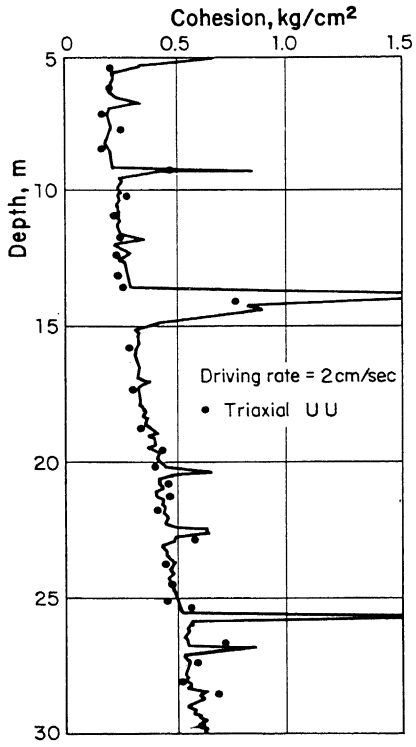


Fig. 8. Cone and Laboratory Undrained Strengths. Section 3

From the triaxial testing program a set of representative stress-strain curves of the soil at the test section was obtained. These curves served to compute average values of the initial tangent modulus, $E_i$, and of the stress ratio, $R_f$. Also, average values of the shear strength, $\sigma_f$, (using the Mohr-Coulomb criterion) and of the unit weight, $\gamma$, were determined. All these parameter values are presented in Table II.

TABLE II. Average Soil Characteristics. Section 3

| Layer | $E_i$ (t/m$^2$) | $R_f$ | $\sigma_f$ (t/m$^2$) | $\gamma$ (t/m$^3$) |
|---|---|---|---|---|
| from 6.0 m to 17.5 m | 550 | 0.90 | 5.6 | 1.2 |
| from 17.5 m to 20.5 m | 570 | 0.90 | 5.8 | 1.2 |

The compressibilities of the soil in its remolded and undisturbed states were evaluated in oedometer tests. Representative samples obtained from the clay layer above the tunnel crown were used in the tests. The resulting compressibility curves for both conditions are depicted in Fig. 9. Again, water content of undisturbed and remolded samples was practically the same.

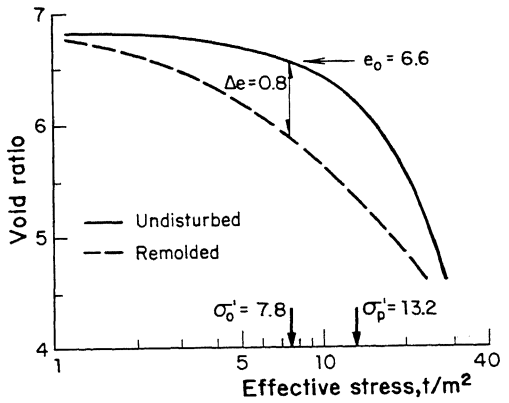


Fig. 9. Representative Compressibilities of Section 3

Instrumentation at this section consisted of eight settlement points distributed in space as shown in Fig. 10. Four of them were installed at a depth of 1.0 m, and the remaining four at 17.5 m. Again, two of the settlement points were located above the tunnel axis and the others at varying horizontal distances as depicted in Fig. 10.

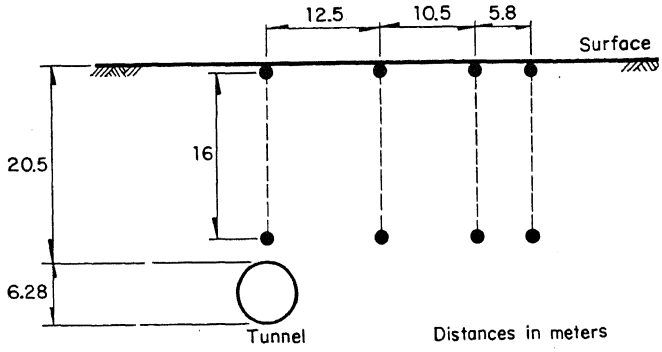


Fig. 10. Spatial Distribution of Settlement Points. Section 3

Section 4

This test section was also located at the intersection of two wide avenues. The subsoil conditions of the site are shown in Fig. 11. The stratigraphic profile is quite similar to those of the other sections: from 0 to about 3 m (not shwon in Fig. 11) hard dissicated sandy clay was found; then comes a layer about 4 m thick of overconsolidated clay followed by a thin layer of sand. Beneath these strata, there is a 23 m thick stratum of normally consolidated clay with intercalated seams of silty clay, fosils, fly ashes, and hardened clay (possibly by dissication). Natural water content varied from 30% to less than 500%; the corresponding water content profile is included in Fig. 11.

Cone and sampling borings were made some ten meters from tunnel axis and about 2 m (in a parking lot) away from the line of settlement points. Cone point resistance was measured at a driving rate of 2 cm/sec. The resulting undrained strength versus depth is depicted in Fig. 12. Alternatively, undrained triaxial tests (UU) were perfomed on undisturbed samples. The resulting undrained shear strengths were correlated with the strengths derived from the cone penetration test. In this case, the correlation parameter N was 17 for soft layers (i.e., cone point resistance less than about 10) and 23 for harder layers (i.e., cone point resistance greater than about 15). The resulting correlation is presented in Fig. 12.

From the triaxial testing program a set of stress-strain curves representing the behavior of the soil was obtained. These curves were the basis to compute average values of the initial tangent modulus, $E_i$, and of the stress ratio, $R_f$. Similarly, mean values of the shear strength, $\sigma_f$, (using Mohr-Coulomb criterion) and of the soil unit weight, $\gamma$, were calculated. These

parameters are presented in Table III.

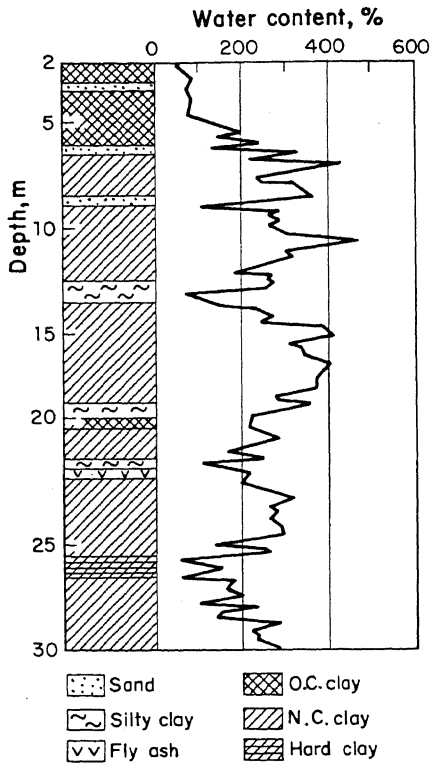


Fig. 11. Soil Profile at Section 4

TABLE III. Average Soil Characteristics. Section 4

| Layer | $E_i$ ($t/m^2$) | $R_f$ | $\sigma_f$ ($t/m^2$) | $\gamma$ ($t/m^3$) |
|---|---|---|---|---|
| from 6.0 m to 17.5 m | 520 | 0.90 | 5.3 | 1.2 |
| from 17.5 m to 20.5 m | 540 | 0.90 | 5.5 | 1.2 |

The compressibilities of the soil in its undisturbed and remolded states were determined in oedometer tests. Representative samples obtained from the clay layer above the tunnel crown were used in the tests. The resulting compressibility curves for both conditions are depicted in Fig. 13. Water content of remolded and undisturbed samples was practically the same.

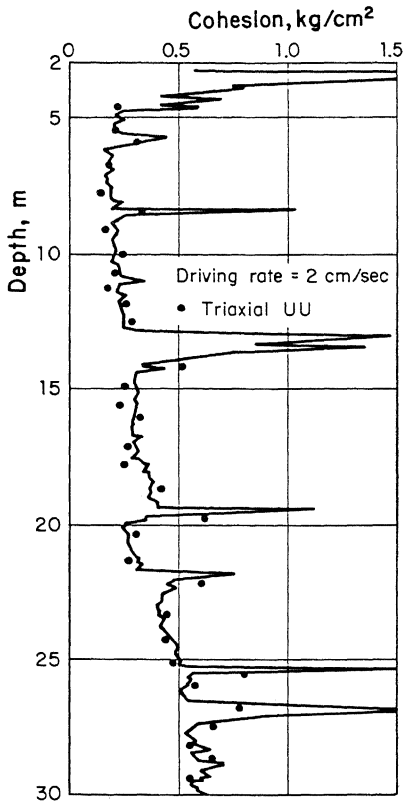


Fig. 12. Cone and Laboratory Undrained Strengths. Section 4

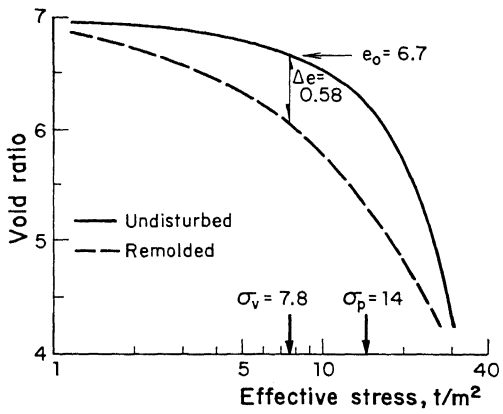


Fig. 13. Representative Compressibilities of Section 4

Instrumentation at this section also consisted of eight settlement points spatially distributed as indicated in Fig. 14. Again, four of the measuring points were buried at a depth of 1 m, and the remaining four at a depth of 17.5 m. As seen in Fig. 14, two settlement points were installed above the tunnel axis and the others at varying horizontal distances.

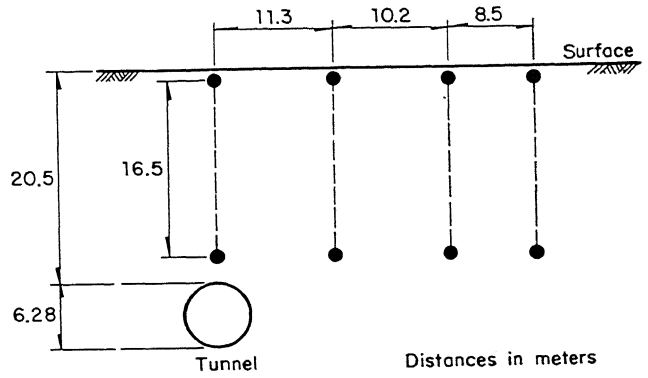


Fig. 14. Spatial Distribution of Settlement Points. Section 4

Section 5

This measuring section was located on a circle traffic. The subsoil conditions of the site are shown in Fig. 15. The stratigraphy is similar to those of the other testing sections: from 0 to 3 m (not shown in Fig. 15) hard dissicated sandy clay was found; then follows a layer about 4 m thick of overconsolidated clay and a thin layer of sand. Underneath these strata, there is a 23 m - thick stratum of normally consolidated clay with intercalated seams of silty clay, fosils, fly ashes, and hardened clay (possibly by dissication). Natural water content ranged between 30% and about 450%; the profile of water content is included in Fig. 15.

From the triaxial testing program a set of stress-strain curves representing the in situ soil behaviour was obtained. These curves served to compute average values of the initial tangent modulus, $E_i$, and of the stress ratio, $R_f$. Similarly, mean values of the shear strength, $\sigma_f$, (using Mohr-Coulomb criterion) and of the soil unit weight, $\gamma$, were calculated. The values of these parameters are presented in Table IV.

The compressibilities of remolded and undisturbed soil samples were determined from oedometer tests. The samples were obtained from the clay layer above the tunnel crown. The resulting compressibility curves for both conditions are shown in Fig. 16. Again, the water content of both types of specimens was practically the same.

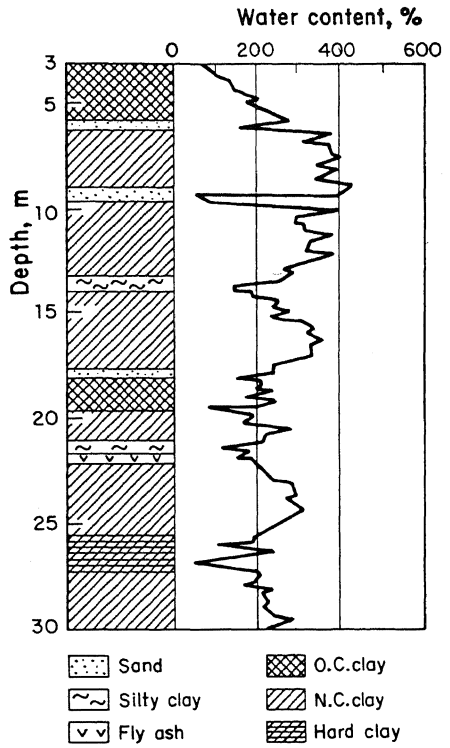


Fig. 15. Soil Profile at Section 5

TABLE IV. Average Soil Characteristics. Section 5

| Layer | $E_i$ (t/m$^2$) | $R_f$ | $\sigma_f$ (t/m$^2$) | $\gamma$ (t/m$^3$) |
|---|---|---|---|---|
| from 6.0 m to 12.0 m | 530 | 0.9 | 5.3 | 1.2 |
| from 12.0 m to 20.5 m | 560 | 0.9 | 5.6 | 1.2 |

Instrumentation at this section consisted of ten settlement points spatially distributed as indicated in Fig. 17. Five measuring points were installed at a depth of 6 m, and the remaining five at a depth of 12 m. In this section, due to the reduced available space for maneuvers it was not possible to locate all the instruments on the same plane. However, for the purpose of interpretation it will be assumed that all the settlement points fall on the same plane perpendicular to tunnel axis.

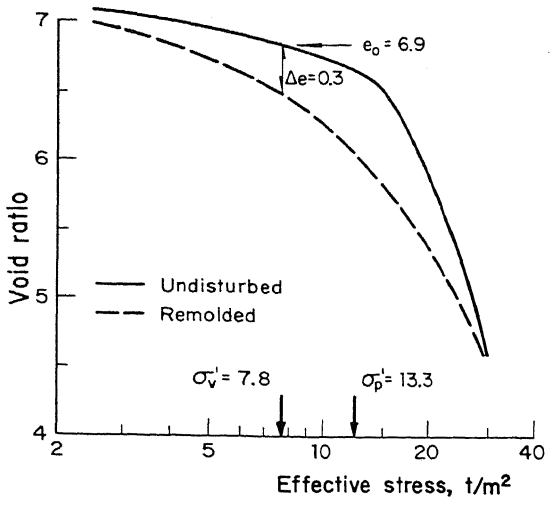


Fig. 16. Representative Compressibilities of section 5

## COMPUTED AND OBSERVED SETTLEMENTS

According to the construction procedure adopted, tunneling-induced settlements are the result of three different mechanisms: a) stress release at tunnel face, b) yielding of tunnel wall to fill the annular gap developed between soil and primary lining, and c) increased compressibility of a ring of soil remolded by tunneling operations. Additional settlments may be caused by further lining deformation upon air pressure release, and ground consolidation resulting from steady-state seapage toward the tunnel. Here, only the settlements induced by direct construction operations (the first three) will be considered.

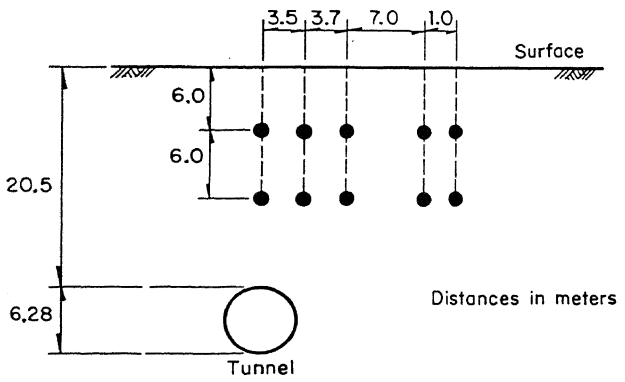


Fig. 17. Spatial Distribution of Settlement Points. Section 5

### Method of Analysis

The theoretical model to compute tunneling-induced settlements in soft ground was first presented by Reséndiz and Romo (1981) and modified later by Romo (1983).

The method of analysis was developed through numerical simulations using a nonlinear, finite element approach. Analytical expressions were developed for computing ground settlements induced by stress release by tunnel face excavation, inward soil movement due to tunnel wall yielding, and consolidation of soil remolded around the tunnel (which corresponds to an additional soil inward displacement).

Solution for these settlement surces can be summarized as follows (Reséndiz and Romo, 1981; Romo, 1983).

Settlement profiles, by stress release at tunnel face, at any depth across tunnel alignment at a given station B are given by Eqs 1 and 2:

$$\lambda_y = \lambda_B \exp\{-\frac{1}{2}\left[y'(1 + 0.1\,n)^{1/n}\right]^2\} \quad (1)$$

$$\lambda_B = D(0.0083-0.0025\,S)(t)^{1/t}(\sigma_h^o-p_i)\frac{3.26}{E_i(1-R_f)} \quad (2)$$

where $\lambda_B$ = settlement above tunnel axis at any station B; z = upward distance measured from tunnel crown depth; D = tunnel diameter; $\sigma_h^o$ = initial horizontal stress at deptn of tunnel axis; $p_i$ = air pressure at tunnel face; $E_i$ = initial tangent modulus; $R_f$ = shear strength ratio; y = horizontal distance from and normal to tunnel axis; y' = y/(z+D); n = z/D; t = (z+H)/(z+D); and S = z/H.

Settlement profiles across tunnel alignment induced at a given station B by inward soil movement (tunnel wall yielding plus consolidation of the ring of remolded soil) can be calculated by Eqs 3 and 4:

$$\lambda_y' = \lambda_o \exp\{-\frac{1}{2}\left[y'\,u^u\right]^2\} \quad (3)$$

$$\lambda_o = \delta\left[1 + \frac{\sigma_f}{E_i(1-R_f)}\,n\right]^{-0.3n} \quad (4)$$

where $\delta$ = total inward displacement (i. e., tunnel wall yielding, $\delta_y$, plus displacement due to consolidation of disturbed soil, $\delta_c$); and u = 1.2 + 0.1n.

The amount of inward displacement due to yielding of tunnel wall, $\delta_y$, is difficult to be evaluated because it depends on the elapsed time since advancing the shield to installation of the primary lining and grouting the gap. For practical purposes, $\delta_y$ may be assumed to have a value equal to a fraction of the tail shield thickness (plus some overcutting and overexcavation due to steering problems) according to surrounding soil stiffness.

Romo et al. (1980) proposed to evaluate the thickness, $\Delta_r$, of the ring of soil "totally" remolded by tunneling operations by means of Eq 5:

$$\Delta_r = \frac{E_i(1-R_f)}{0.6\ \sigma_f}\ \delta_y \qquad (5)$$

Changes in soil compressibility due to remolding can be assessed by means of oedometer tests on disturbed and undisturbed equivalent soil samples. Once compressibility curves are obtained, the inward displacement due to consolidation of remolded soil, $\delta_c$, can be calculated using the equation,

$$\delta_c = \frac{\Delta e}{1 + e_o}\ \Delta_r \qquad (6)$$

where $\Delta e$ = void ratio change at constant overburden load, upon soil remolding; and $e_o$ = void ratio at initial overburden load at tunnel crown elevation . Ground settlements resulting from inward soil displacement are computed replacing $\delta$ by $\delta_y$ plus $\delta_c$ in Eq 4.

Total settlements at any depth caused by the overall effect of these components are calculated adding up each contribution from Eqs 1 and 3.

## COMPUTED AND OBSERVED TOTAL SETTLEMENTS

The method of analysis allows computation of the settlements that may be induced by tunneling at different construction stages. When tunnel excavation was carried out near the instrumented sections, surveying was performed twice a day (the tunnel construction advance was about 6 m per day) with the purpose of being able to identify the various settlement sources. Measurements and computations of settlements for each of the above mentioned components have been compared elsewhere (Romo, 1983) and is beyond the reach of this paper. Here, only the observed and theoretical total settlements are compared.

From the subsoil conditions presented at each test section it may be concluded that the sites are similar and that, for the sake of comparison, all them can be grouped into only one site with settlement points at three depths: 1, 6-6.5, 12-12.5, and 17.5 meters.

The total settlements (caused by the three sources discussed) measured at the four depths are shown in Figs. 18-21. It may be seen that the differences among the profiles are small, and they fall within the scatter it may be expected in this kind of studies. The corresponding theoretical settlements were computed using the average values shown in Table V. The resulting settlements are shown in Figs. 18-21 with solid lines.

These results show that the settlements calculated by Eqs 1-4 agree quite well with the settlements measured throughout the whole zone of tunneling influence.

TABLE V. Parameters Used in Analyses

| | | |
|---|---|---|
| Tunnel Diameter, D | 6.28 | m |
| Crown Depth, H | 20.50 | m |
| Initial Horizontal Stress, $\sigma_h^o$ | 20 | $t/m^2$ |
| Air Pressure, $p_i$ | 9 | $t/m^2$ |
| Coefficient at Rest, $K_o$ | 0.7 | |
| Unit Weight, $\gamma$ | 1.2 | $t/m^3$ |
| Initial Tangent Modulus, $E_i$ | 580 | $t/m^2$ |
| Strength Ratio, $R_f$ | 0.90 | |
| Shear Strength, $\sigma_f$ | 5.7 | $t/m^2$ |
| Vertical Effective Stress, $\sigma_v'$ | 7.8 | m |
| Tunnel Wall Yielding, $\delta_y$ | 0.08 | m |
| Initial Void Ratio, $e_o$ | 6.6 | |
| Void Ratio Change, $\Delta e$ | 0.5 | |

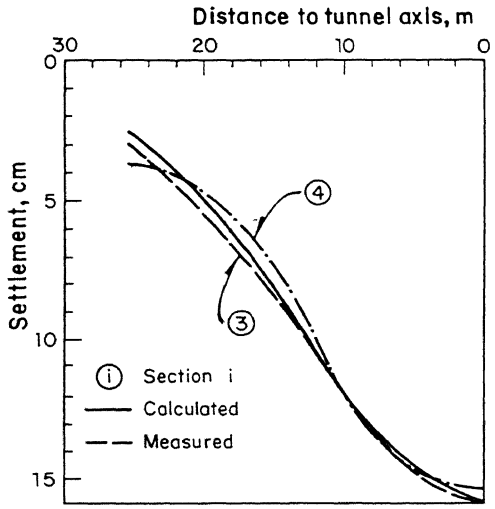


Fig. 18. Total Settlement at 1 m Deep

## CONCLUSIONS

The results of a program to monitor the settlements caused by the construction of a sewerage tunnel in soft clay are presented. Five observation sections were set up along the 1888 m-long tunnel. The instrumentation consisted of shallow and deep settlement points arranged in such a way that settlement profiles could be adequately defined.

The subsoil conditions and the results of field and laboratory testing programs indicated that the five sites could be (for comparison purposes) reasonably well characterized by one section having the average stratigraphy and soil properties of the five. Accordingly, all the settlement profiles measured can be interpreted as if they had been measured at one site but at four different elevations.

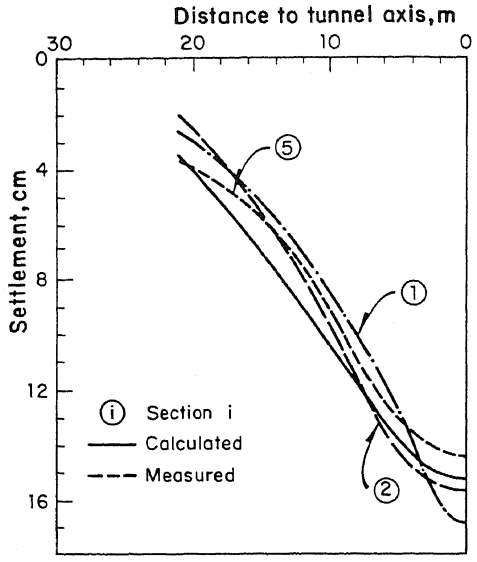


Fig. 19. Total Settlements at 6-6.5 m Deep

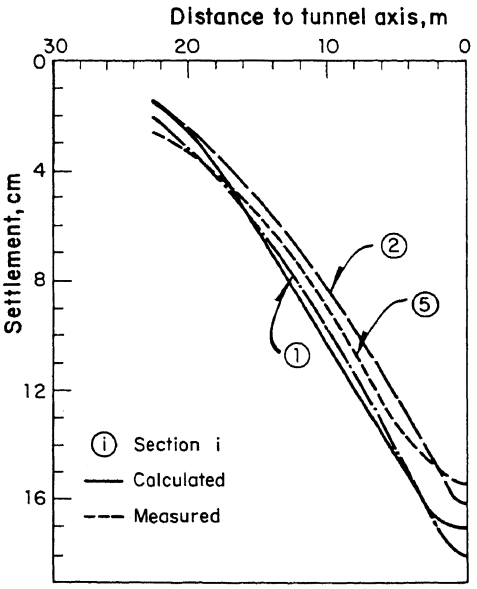


Fig. 20. Total Settlements at 12-12.5 m Deep

Comparisons between computed and measured settlement profiles clearly show the excellent accuracy of the simplified method of analysis. Henceforth, it seems that this approach can be confidently used to forecast vertical movements induced by tunneling operations in soft ground. Consequently, use of this approach prior to construction may help the engineer to make some adjustments to the design or construction procedure. Alternatively, for given tunnel construction procedure and subsoil conditions, the spatial distribution of settlements can be predicted and potential damage to neighboring structures and services assessed. It is understood that to better evaluate structural damage a more complete soil movement field is required. To this end, a similar approach to compute horizontal displacements (presently under verification) has been developed by the author in the recent past.

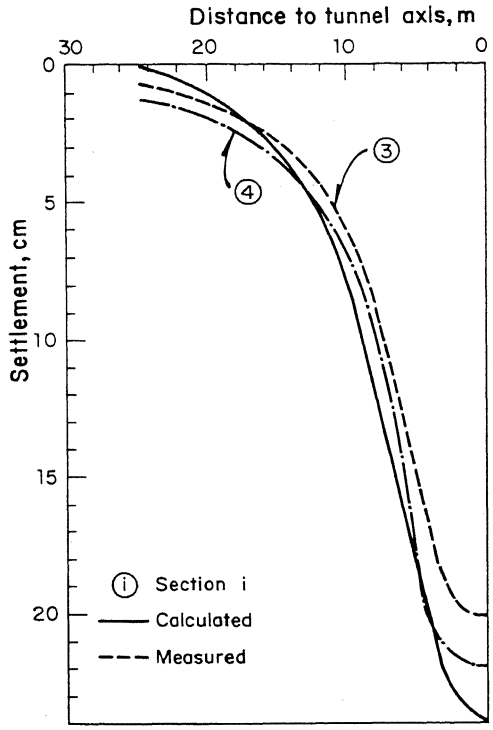


Fig. 21. Total Settlements at 17.5 m Deep

REFERENCES

Attewell, P. B. (1981), Engineering Contract, Site Investigation and Surface Movements in Tunnelling Works. In Soft-Ground Tunneling: Failures and Displacements. Ed. by Reséndiz and Romo, A. A. Balkema, Rotterdam

Marsal, R. J. and M. Mazari (1959), El Subsuelo de la Ciudad de México. Contribution of Instituto de Ingeniería. First Pan American Conference in Soil Mechanics and Foundation Engineering, México

Reséndiz, D. and M. P. Romo (1981), Settlements upon Soft-Ground Tunneling: Theoretical Solution. In Soft-Ground Tunneling: Failures and Displacements. Ed. by Reséndiz and Romo, A.A. Balkema, Rotterdam.

Romo, M. P., C. Díaz and D. Reséndiz (1979), Método para Estimar Asentamientos Causados por la Construcción de un Túnel en Suelos Blandos. Instituto de Ingeniería, Report to Dirección General de Construcción y Operación Hidráulica, D. D. F., México

Romo, M. P., C. Díaz and A. Luna (1980), Remoldeo Inducido por la Construcción de un Túnel con Escudo. Instituto de Ingeniería, Report to Dirección General de Construcción y Operación Hidráulica, D.D.F., México

Romo, M. P. (1983), Asentamientos Inducidos por Tuneleo en Suelos Blandos. Instituto de Ingeniería. Report to Dirección General de Construcción y Operación Hidráulica, D.D.F., México

Schmitter, J. M., P. D. Farjeat and A. H. Canseco (1981), Soft-Ground Tunneling in Mexico City. Proc. of the 1981 Rapid Excavation and Tunneling Conference. San Francisco, Cal., 801-812